RD No. SE-5
RL No. 139

LARGE AREA SHEET TASK

JPL NO. 9950-605

ADVANCED DENDRITIC WEB GROWTH DEVELOPMENT

Quarterly Report

April 1, 1981 to June 30, 1981

C. S. Duncan, R. G. Seidensticker, J. P. McHugh,
R. H. Hopkins, D. Meier, and J. Schruben

DOE/JPL-955843/81/3
DIST. CATEGORY UC-63

Contract No. 955843

October 6, 1981

The JPL Low-Cost Silicon Solar Array Project is sponsored by the U. S. Dept. of Energy and forms part of the Solar Photovoltaic Conversion Program to initiate a major effort toward the development of low-cost solar arrays. This work was performed for the Jet Propulsion Laboratory, California Institute of Technology by agreement between NASA and DOE.

Westinghouse R&D Center
1310 Beulah Road
Pittsburgh, Pennsylvania 15235

TABLE OF CONTENTS

LIST OF FIGURES

1. SUMMARY

Silicon dendritic web is a single crystal ribbon form of silicon capable of fabrication into solar cells with AM1 conversion efficiency in excess of 15%. This is the third Quarterly Report under JPL Contract 955843.

During this quarter, three major work areas were emphasized: 1) Development and application of the thermal model for calculating buckling stresses as a function of temperature profile in the web, 2) systematic evaluation of lid and shield concepts to provide the data base for enhancing growth velocity, and 3) the design and construction of a new experimental web growth machine which embodies in one unit the mechanical and electronic features developed in previous work. In addition, evaluation of the new melt level control system was begun, along with preliminary tests of an elongated crucible design. The economic analysis was also updated to incorporate some minor cost changes.

The initial applications of the thermal model to a specific configuration gave results consistent with experimental observation in terms of the initiation of buckling vs. width for a given crystal thickness.

A recessed lid design has been tested and found to exhibit simultaneously some of the advantages of both thick lids (quality of growth) and thin lids (more open view factor and higher velocity).

Both the mechanical and electronic designs of the new experimental web growth machine are complete, purchased components ordered and fabrication is in progress.

The melt level control system has been tested during web growth and some minor but desirable modifications identified.

2. INTRODUCTION

This is the third Quarterly Report on JPL Contract No. 955843 entitled "Advanced Dendritic Web Growth Development." The overall objective is to investigate and develop an understanding of the critical parameters involved in the growth of wide thin long web crystals at high rates of crystallization, and to demonstrate the key results. This effort is fundamental to the ultimate objective of demonstrating the ability of the silicon dendritic web process to produce sheet material at a cost compatible with the DOE/JPL goal of $0.70 per peak watt of photovoltaic output power in 1986.

Silicon dendritic web is a ribbon form of silicon grown directly from the melt without dies or shapers and which produces solar cells with AM1 conversion efficiencies above 15%. Most of the technical requirements to meet the 1986 cost goals have already been demonstrated.

The thrust of this program is to further investigate each critical parameter to learn how it may be improved, combine the results so that the total process may be improved, and to design, fabricate and operate an experimental web growth machine which embodies the combination of the most recent developments in web growth technology.

This report covers the second quarter of 1981, during which major strides were made in the application of thermal modeling to the understanding of stress and buckling phenomena, a new class of lid and shield configurations was systematically investigated, and the construction of a new experimental web growth machine was begun.

3. TECHNICAL PROGRESS

3.1 Stress and Buckling Calculations

3.1.1 WECAN Computer Code

In the last quarterly report [1], we described some aspects of the Westinghouse proprietary finite element computer code, WECAN. In particular, we described the variable-sized grid we set up to model silicon ribbon stresses with the WECAN code. The finite elements delineated by this grid can be of several different types: linear, quadratic or cubic, and either two-or three-dimensional. Linear elements have nodes at every corner, while quadratic and cubic elements have, respectively, one and two additional nodes along the edges joining pairs of corners. Although the higher order elements require more computer time per element, fewer elements are necessary to model the ribbon accurately. Our previous program modeled ribbon stresses on WECAN with two-dimensional linear equally spaced elements [1]. Two-dimensional elements are sufficient for thin silicon ribbon, but the buckling option on WECAN requires three-dimensional elements which are usually of the quadratic type.

Buckling occurs as a sudden deformation in the planar silicon strip when the thermal stresses reach some critical magnitude. Mathematically, buckling can be represented as an eigenvalue problem where the critical stress distribution is represented by an eigenvalue and the buckled shape by an eigenvector. For buckling problems, WECAN solves an equation of the form

$$[K]\ \{\Delta\} = \lambda\ [K_s]\ \{\Delta\} \qquad (1)$$

where [K] is the conventional stiffness matrix, $[K_s]$ is the initial stress matrix resulting from a given temperature distribution, and $\{\Delta\}$

is a vector containing the unknown displacements of the ribbon surface. A solution parameter to the above equation, λ, is an eigenvalue and the corresponding $\{\Delta\}$ is an eigenvector; there can be many eigenvalues for a given equation. The smallest positive one is the most significant, since the product of it with $[K_s]$ is the weakest stress distribution for which buckling occurs. Negative eigenvalues imply a reversal of the sign of the stress distribution or a heating instead of a cooling of the ribbon from the melt surface. Although negative eigenvalues may be obtained mathematically for some $[K_s]$, they are not physically meaningful. We shall discuss these concepts further in terms of a specific example -- ribbon grown using the J181 lid and shield configuration.

3.1.2 Stress Buckling in J181 Ribbon

J181 ribbon is grown out of a silicon melt covered and shielded as illustrated in Figure 1. The corresponding thermal model is shown in Figure 2; the temperatures are measured data [2]. A previously developed thermal modeling program [3] was used to calculate the temperature distribution in the growing web resulting from this growth geometry; the result is shown in Figure 3.* This temperature distribution was used as the input to WECAN to calculate the stresses in a 10 cm long and 150 μm thick ribbon. The width of the web between the dendrites was taken as 2.5 cm for a total ribbon width of 2.7 cm. The WECAN code then calculated the x stress along the length of the ribbon, the y stress across the width of the ribbon, and the xy shear stress. Figure 4 shows the stress contours for these three components. The top edge of the strip is the outer edge of the dendrite, the left edge is the melt surface, the right edge is 10 cm from the melt surface, and the bottom edge is the centerline of the ribbon with the stresses symmetric about this line. These stresses determine the matrix $[K_s]$ of Equation (1), since other components of the stress tensor vanish for thin ribbons.

*Only temperature for distances less than 10 cm from the melt was calculated using the previous program. An asymptotic procedure, to be discussed later, was used for greater distances.

Dwg. 7702A61

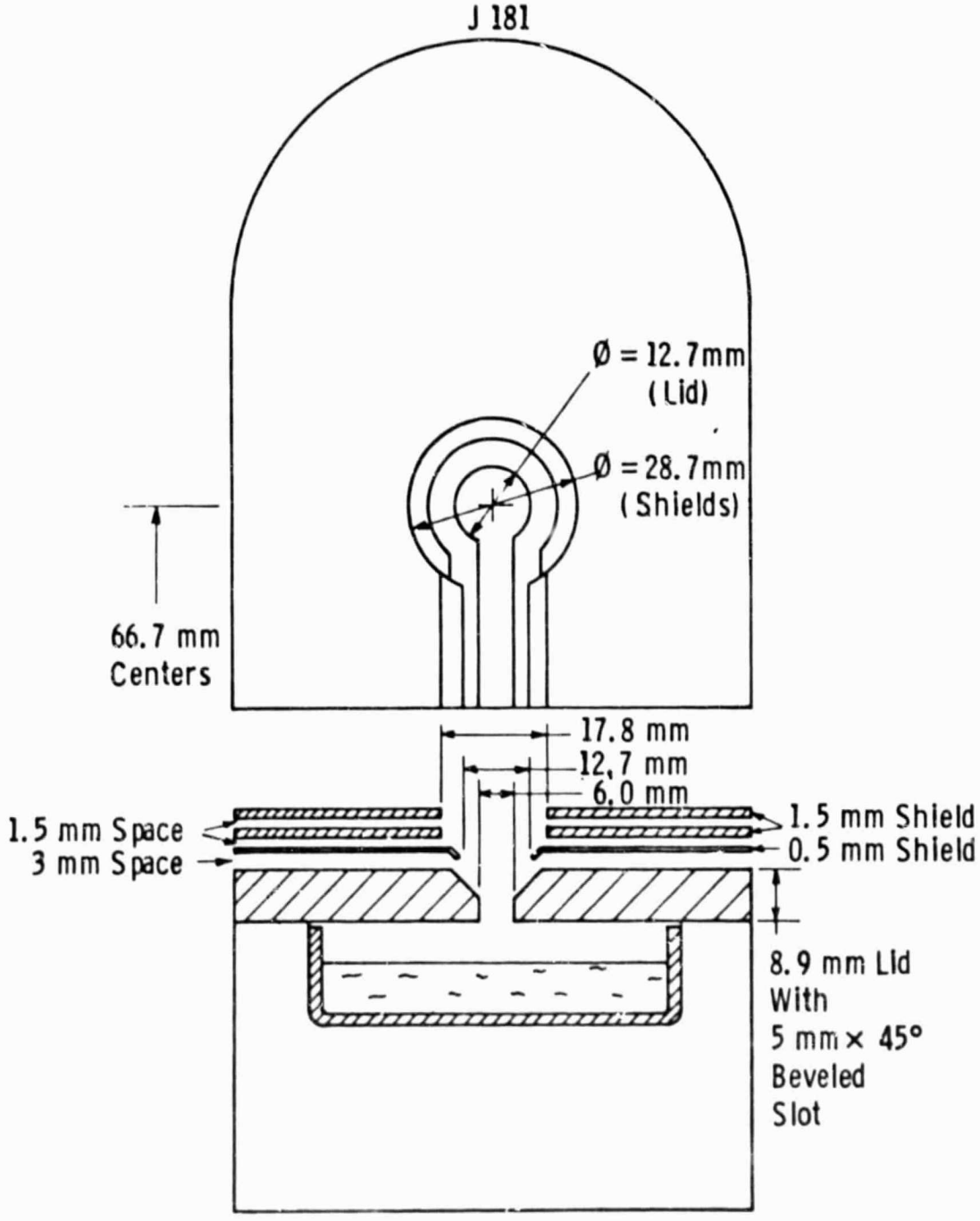

Figure 1 The J-181 Baseline Lid and Top Shield Configuration

Dwg.7709A12

TC	TS	TBEVEL	TAS	TLID	ZD	ZH
1623	1460	.6	1213	1.0	1.35	1.85

Dimensions in CM

Temp. in °K

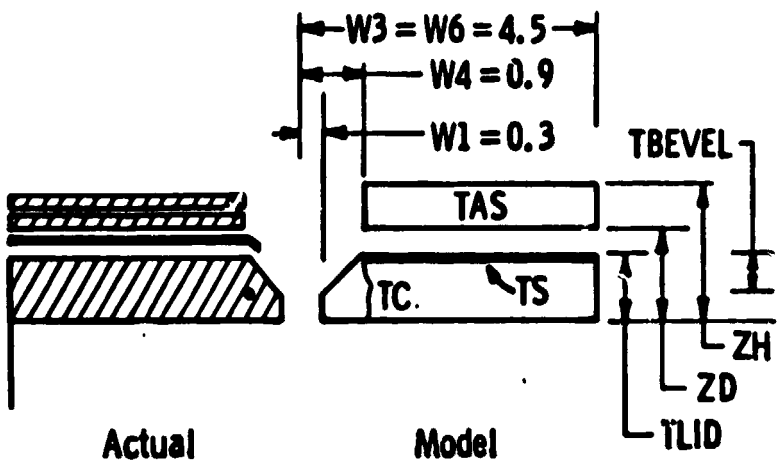

• Thermocouple Location

Figure 2 J181 Thermal Model

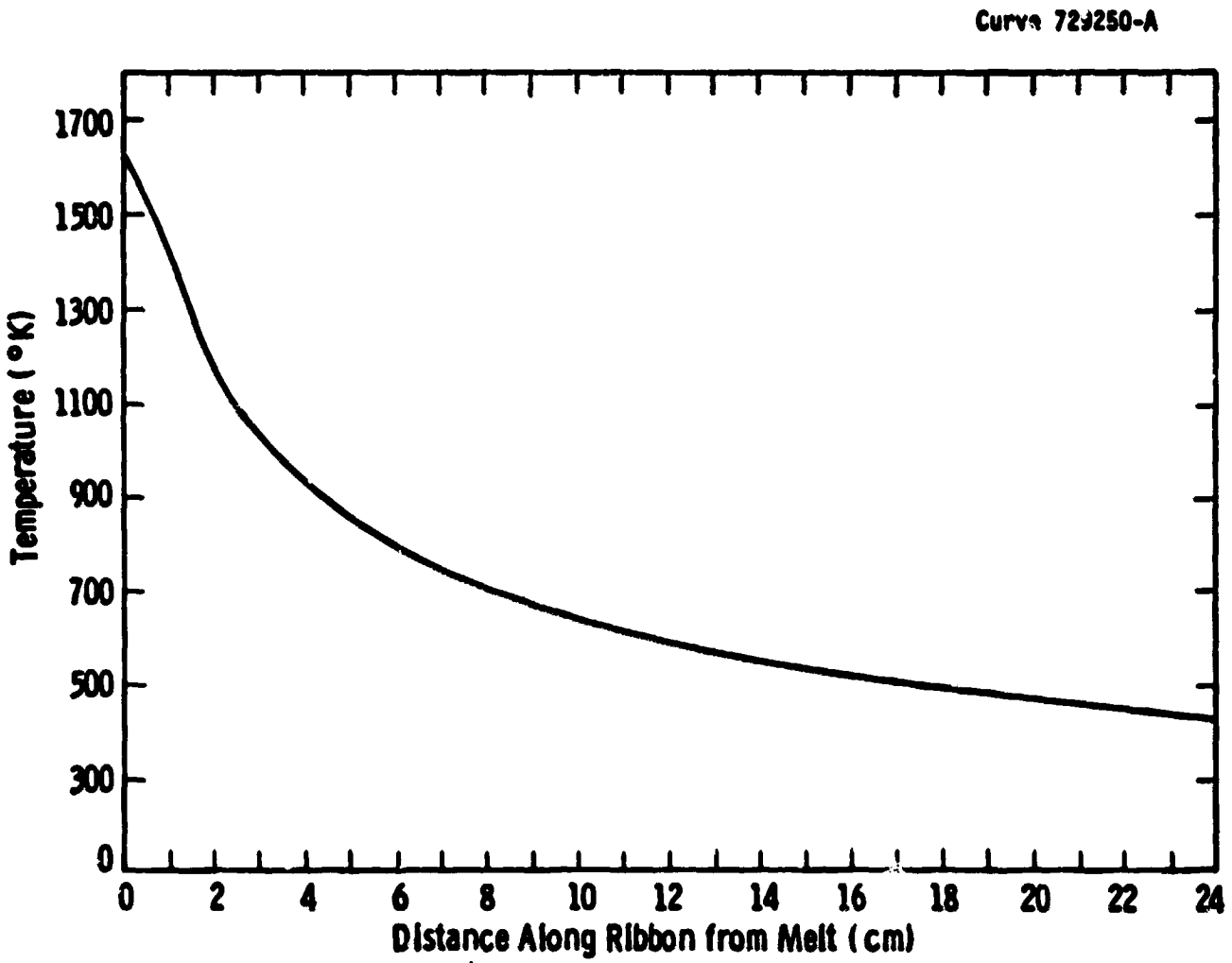

Figure 3 J181 Thermal Profile

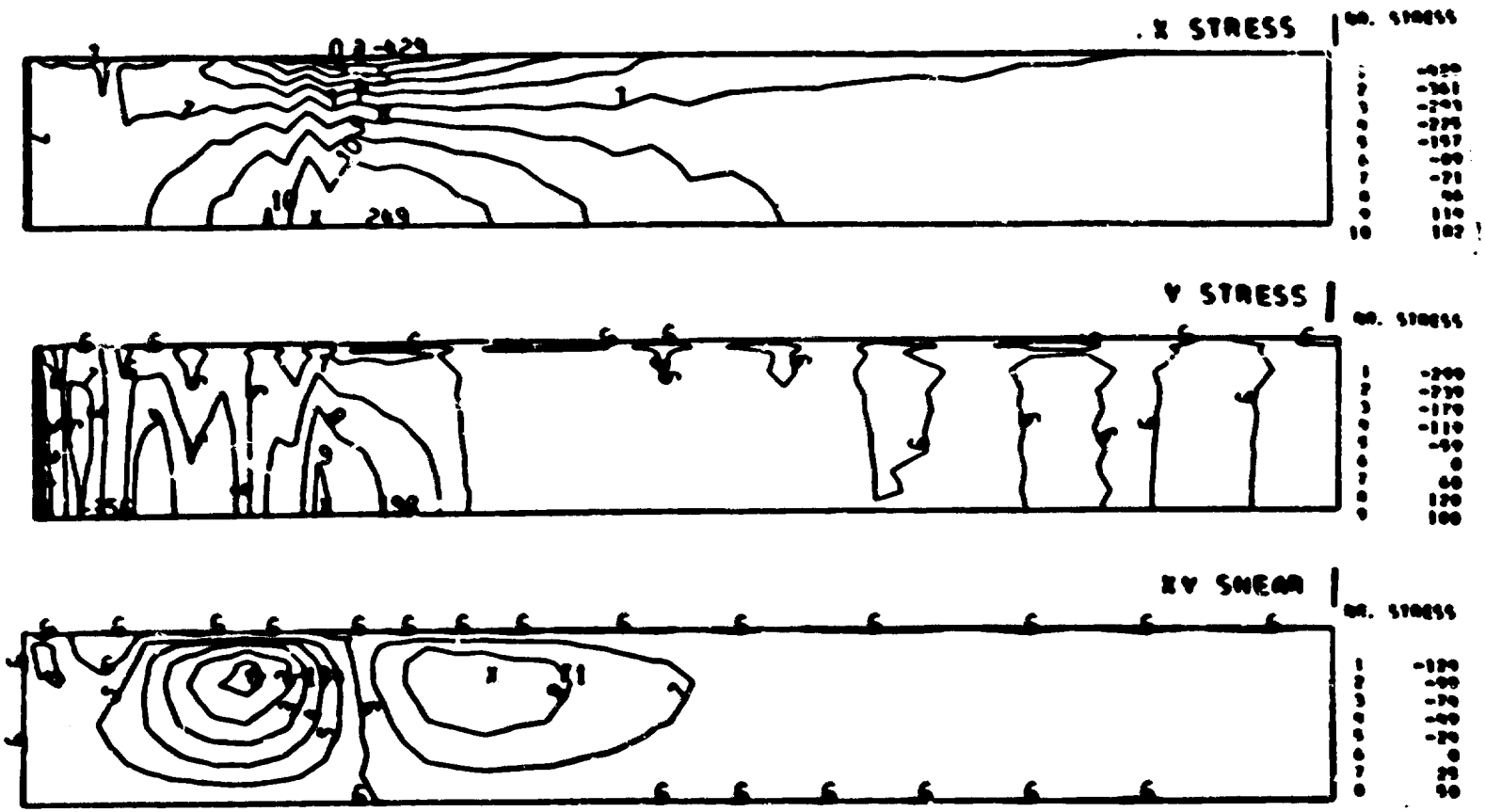

Figure 4 Stress distribution in 27 mm "J181" web

Using the initial stress matrix $[K_\sigma]$, WECAN then solved Equation (1) for the eigenvalue $\lambda = 1.65$ and its corresponding eigenvector or buckled shape is illustrated in Figure 5. Since λ is greater than unity, this ribbon would not have buckled — all the stresses would have to be increased by a factor of 1.65 to obtain the illustrated deformation. The stability of 150 μm thick and 27 mm wide web agrees with growth experience with the J181 configuration.

In the actual growth apparatus, the ribbon is actually about 50 cm long rather than 10 cm before it is wound up on the reel. The computer used for the WECAN analysis does not have sufficient storage capacity to model this length unless it were divided up into very large elements. Since the largest stresses occur within only about 3 cm of the melt interface, it was felt that a 10 cm long model would be adequate for the present purposes. Nevertheless, we added three rows of elements for a total length of 13.6 cm to check the invariance of the eigenvalue λ. This longer ribbon was found to require slightly more stress for buckling with $\lambda = 1.67$. We felt that this 0.02 increase in λ was within experimental error and insufficient to warrant the additional computer time.

Not only is more computer time necessary to evaluate longer models, but the temperature input data is more difficult to obtain. The temperature integration becomes inaccurate at large distances away from the melt surface. An asymptotic method was used to find the temperature of the ribbon away from the melt as graphed in Figure 3. This method will be discussed in an appendix to a future support.

3.1.3 Investigation of Buckling Parameters

With some assurance that the WECAN buckling model is reasonable, we proceeded to use it to investigate the effect of ribbon width and thickness on the buckling resistance. These parameters are of prime importance in the eventual goal of designing a growth geometry which will grow wide, thin (i.e., fast) web crystals.

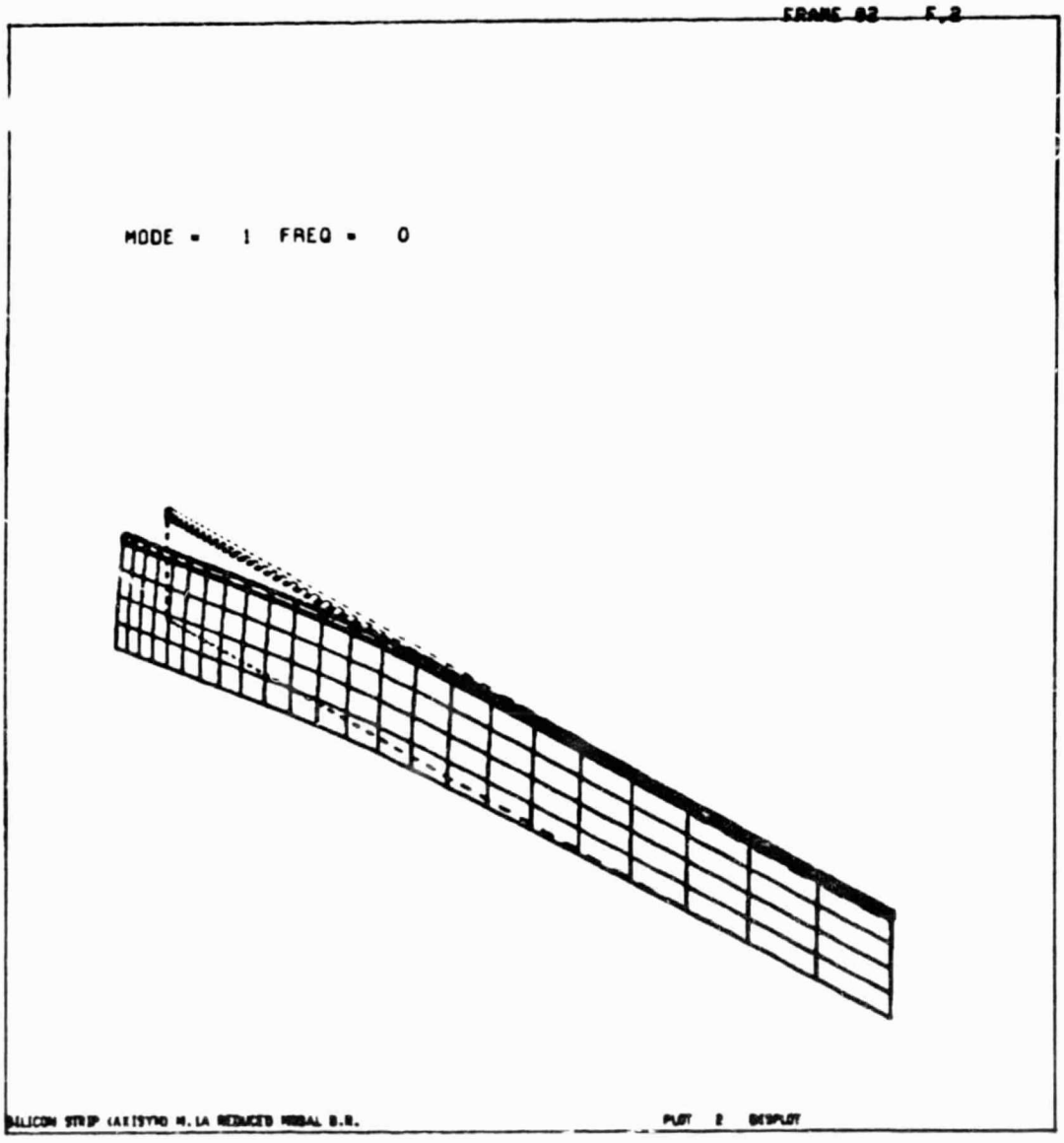

Figure 5 Calculated shape of buckled web (half strip).

3.1.3.1 Width Effects

We chose two widths, 33mm and 39.5mm, to compare with the 27 mm J181 ribbon which was initially modeled. The stress contours for these widths are shown in Figures 6 and 7. According to Boley and Wiener's approximation [4], the shear stress should vanish on the centerline and it does in the numerical results. The x- and y-stresses, however, do not exhibit the expected width dependence: $\sigma_x \sim w^2$ and $\sigma_y \sim w^4$. Examining the point of maximum stress along the centerline, we find instead that $\sigma_x \sim w^{.91}$ and $\sigma_y \sim w^{1.28}$ with a slight variation in the exponent depending on which of the width cases are compared. The fact that the exponent is not equal to 2 for the x-stress is not too surprising since Boley and Wiener's approximation [5] is best at distances far away from the ends of a ribbon, whereas in our case the maximum stress is only about a ribbon width away from the melt end. For this same reason, it cannot be expected that the x-stress at the dendrite edge should be double that at the centerline and opposite in sign as predicted by the approximate theory [4]. It is also true that the dendrites affect the stress pattern. The ratios of the minimum x-stress on the dendrite edge to the maximum x-stress on the centerline are -1.7, -1.8 and -1.9 for the 27 mm, 33 mm and 39.5 mm widths of ribbon, respectively. The increasing magnitude of this ratio for increasing widths probably reflects the decreasing stiffness effect of the dendrite since the dendrite width is held constant at 1 mm.

The smallest positive eigenvalues for the 33 and 39.5 mm ribbons are $\lambda = 0.797$ and $\lambda = 0.418$, respectively. Their corresponding eigenvectors (shapes) are very similar to that shown in Figure 5. Since these eigenvalues are less than unity, the ribbon would buckle before its width could be increased from 27 mm to 33 mm. If we assume that λ varies inversely as the n_{th} power of the width, then $n = 3.63$ for a comparison of the 27 mm and 33 mm widths; using $n = 3.63$ to interpolate we find that the ribbon should buckle ($\lambda = 1$) at $w = 31$ mm. This agrees well with growth experience for web crystals grown from a J181 configuration.

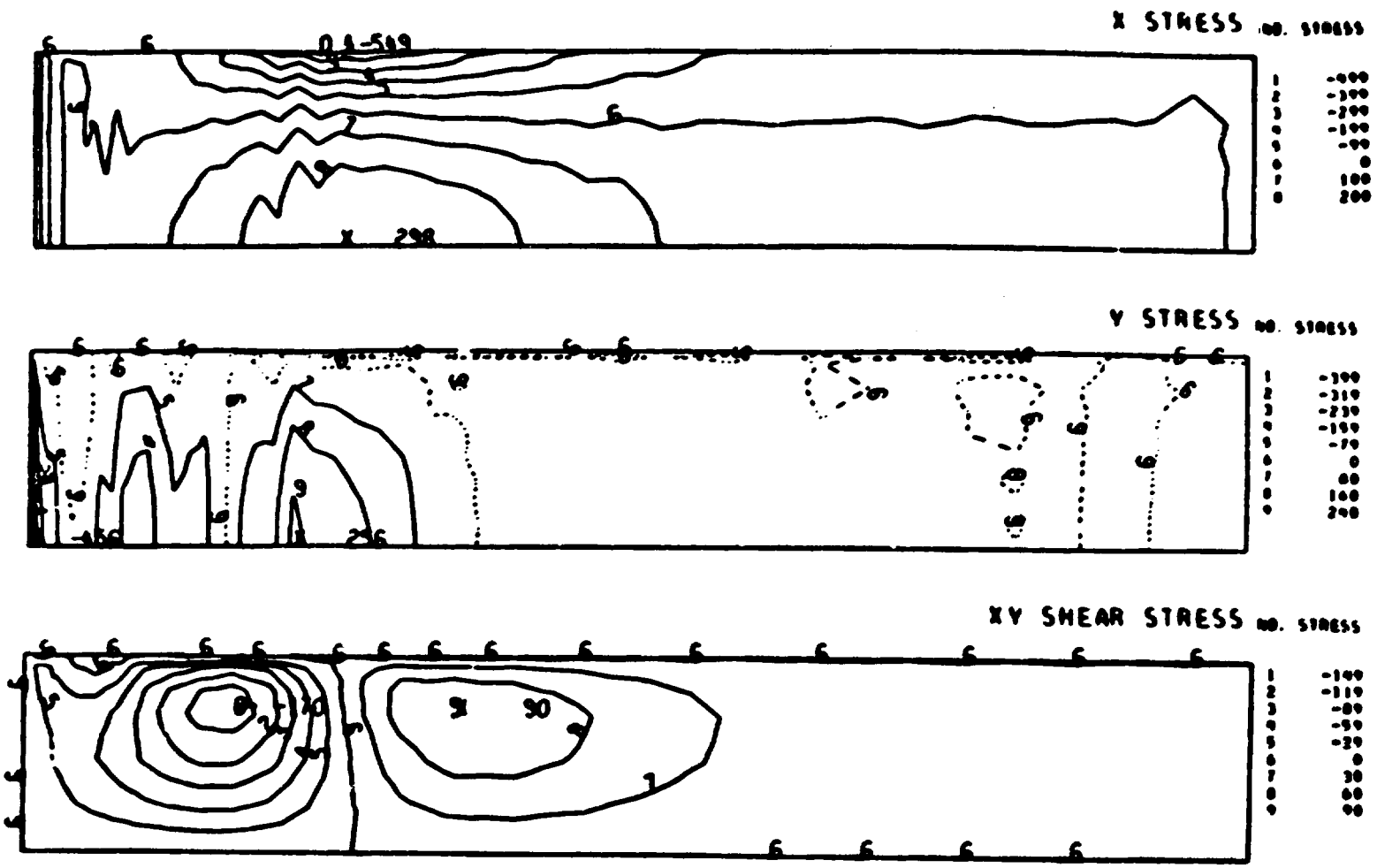

Figure 6 Stress distributions for 33 mm "J181" web

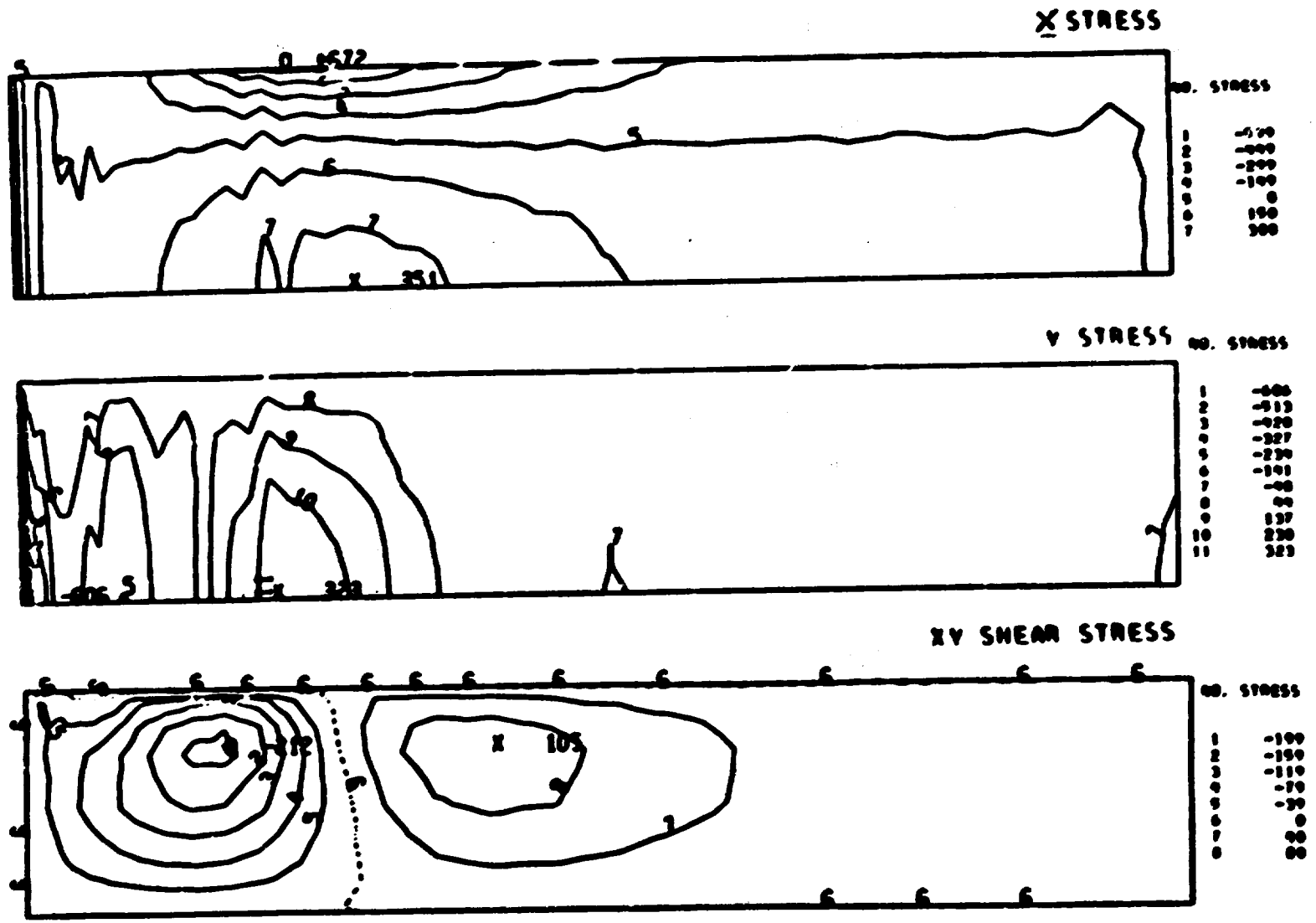

Figure 7 Stress distributions for 39.5 mm "J181" web

The 39.5 mm ribbon has another eigenvalue less than unity: $\lambda = 0.95$. Its buckled shape is pictured in Figure 8. This wide ribbon could buckle like this or in the shape of its first order mode ($\lambda = 0.418$). The first order mode is the more likely one to occur with the higher order mode occuring only if physical constraints should damp the lower mode.

3.1.3.2 Thickness Effects

We evaluated two additional ribbon sizes: 100 μm thick by 27 mm wide and 300 μm thick by 39.5 mm wide. From plots of the stress distributions, we find that the ratios of minimum to maximum x-stress are -1.4 for the smaller and -2.3 for the larger ribbon. In the 300 μm by 39.5 mm ribbon, the minimum x-stress does not occur at the same distance from the melt surface as that of the maximum x-stress. For this case, if we choose a point on the dendrite at the same distance from the melt as the point where the maximum x-stress occurs on the centerline, then the ratio of dendrite to centerline stress is -2.1, which is very close to the predicted value of -2. Again we find that the ratio of dendrite to centerline stress is closest to -2 in those ribbons in which the dendrites have the least volume relative to the rest of the ribbon. The difference between the thickness of the dendrite and that of the ribbon remains constant as the ribbon thickness is varied, so that the dendrite's relative volume is smallest for wide, thick ribbons.

The smallest eigenvalue for the 100 μm by 27 mm ribbon is 1.11, while that for the 300 μm by 39.5 mm ribbon is 1.06. Thus the 27 mm wide ribbon would buckle when its thickness decreases to some value less than 100 μm, and the 39.5 mm ribbon would buckle at some critical value between 150 μm and 300 μm. To determine the critical thickness, we interpolate using the assumption that the eigenvalue λ is proportional to the mth power of the thickness; for our cases, $m = 0.98$ for the 27 mm ribbon and $m = 1.34$ for the 39.5 mm wide ribbon. Using these m's, we find that the 27 mm ribbon should buckle at 90 μm and the 39.5 mm ribbon should buckle at 287 μm. These points, together with the 150 μm thickness for a 31 mm width are plotted in Figure 9. The regions of stability (thick or narrow

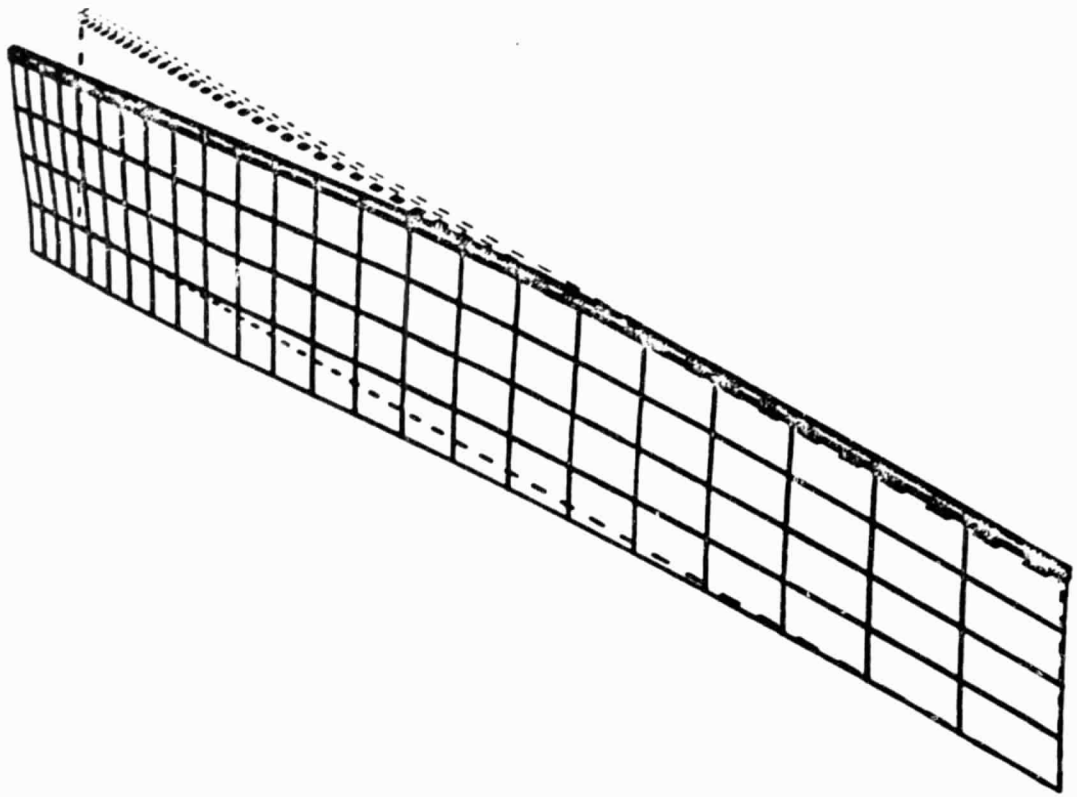

Figure 8 Buckled shape for 39.5 mm "J181" web (second eigenvalue)

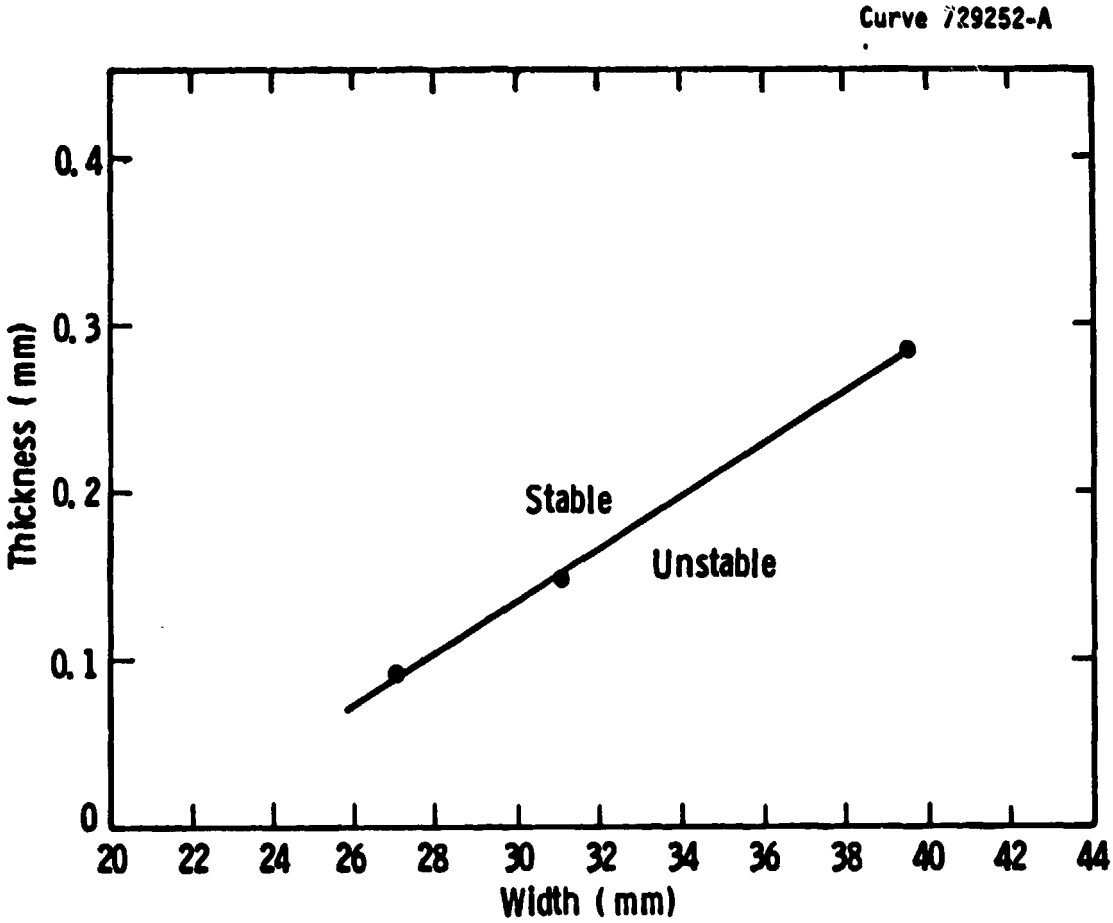

Figure 9 Buckling as function of width and thickness for J181 lid configuration

web) and instability (wide or thin web) are separated by an essentially straight line. Points determined by calculating the width at which a 100 μm or 300 μm thick web would buckle also lie on this line. The simplicity of this result is rather surprising in light of the complexity of the buckling mechanism.

3.1.4 Temperature Profiles for Zero Stress

We have seen that the J181 configuration produces a temperature profile along the ribbon that would cause sufficient stress to buckle silicon ribbon grown to a 31 mm width and 150 μm thickness. In order to redesign the lid and shield configuration to produce wider and/or thinner ribbon, we would like to know how the temperature profile could be modified to reduce stresses in the ribbon. A first step toward this goal is to find temperature profiles that produce no stress at all.

That a linear temperature profile should yield zero stress is derived from the equation

$$\Delta^2 \phi = \alpha E \Delta T$$

where ϕ is Airy's stress function, α is the thermal expansion coefficient, E is Young's modulus and Δ is Lapalace's operator[6]. For zero stress, the left hand side vanishes and we find that $T''(x) = 0$, since T is a function only of the distance x from the melt and not of y or z (to a close approximation in ribbon growth). The above equation, however, was derived for constant α. For α a function of T ($\alpha = 2.8171 \times 10^{-6} + 9.789 \times 10^{-10} T$ for silicon), we replace the condition $T'' = 0$ by $(\alpha T'') = 0$. One resulting temperature profile is shown in Figure 10, curve 9-1. This curve must pass through the point ($x = 0$, $T = 1685°K$) and can be at any chosen temperature at the other end. However, if this temperature is reasonable, then the slope at $x = 0$ would be so small as to produce very slow ribbon growth. If the initial slope of this curve were chosen for reasonable speed, then the temperature at the other end of the ribbon would be so low as to be physically impossible. One way around this problem is to try to design for a "zero stress" temperature profile

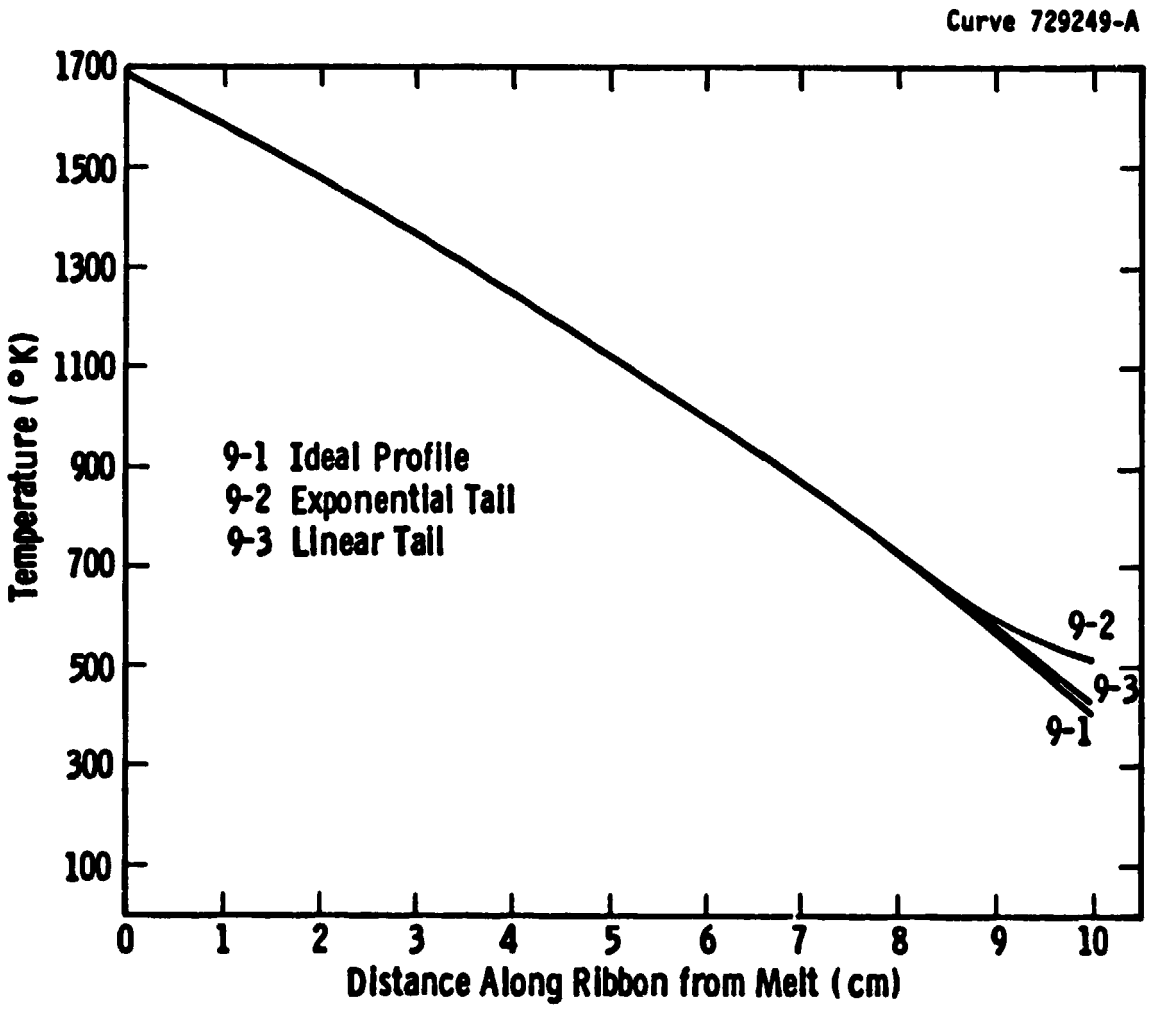

Figure 10 Synthetic temperature profiles

near the melt with a reasonable slope and then, at some point far from the melt, decrease the temperature at a much slower rate than that of the "zero stress" profile.

In Figure 10, curve 9-1 is a "zero stress" curve. At 8 cm from the melt, two "tails" were joined to this curve in such a way as to maintain a continuous first derivative. The "tail" 9-3 is linear and 9-2 is an exponential function of x.

Plots of the difference in longitudinal stress (σ_x) between the centerline and the dendrite edge for each of the three temperature profiles are shown in Figure 11. The linear tail, which is barely distinguishable from the "zero stress" tail, produces a small additional stress. The exponential tail produces a major stress peak at about 8.5 cm from the melt, although it is not nearly as strong as some of the J181 cases which peaked at close to 1000 Mdyn/cm^2. The "zero stress" profile appears to produce small stresses at both ends of the ribbon; this is an artifact of the model. For these three cases, an 8x100 mesh of linear, two-dimensional, finite elements was used to model the half-strip. The "zero stress" case was additionally modeled with a 5x23 mesh of cubic finite elements which have eight more nodes per element than the linear elements. The calculations using the cubic elements gave a zero stress over the whole ribbon length and incidently took much less computer time.

3.1.5 Summary and Future Plans

We have found that small deviations from the ideal "zero stress" temperature profile can produce major stresses in a ribbon. To understand and quantify this effect better, we plan to examine additional synthetic temperature profiles for stress generation. In particular, profiles with steeper slopes at the melt surface are required for reasonable growth speeds.

We have also determined a nearly linear relationship between width and thickness for the conditions at which a web will buckle when grown in a J181 configuration. We next plan to investigate another

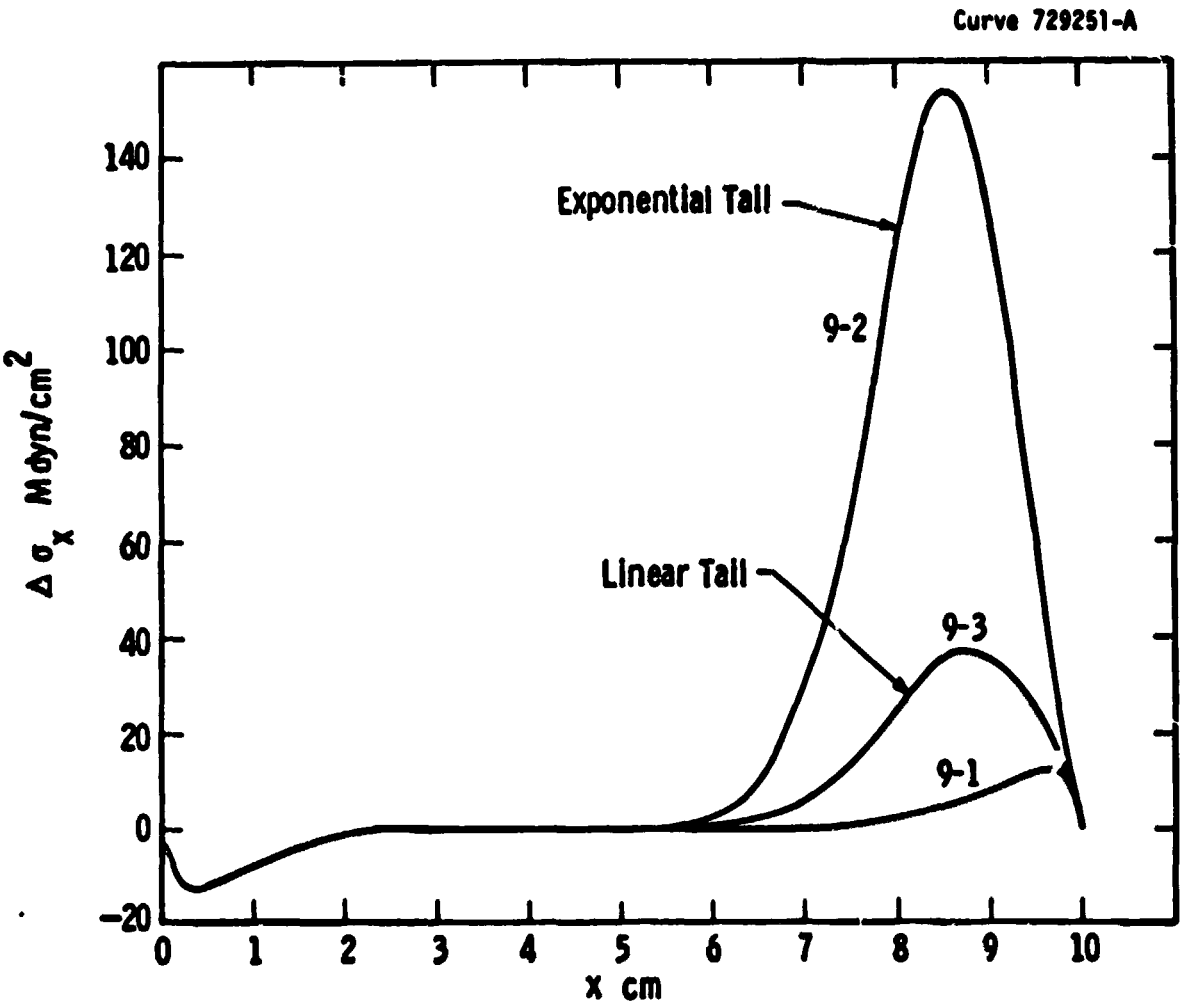

Figure 11 Comparison of stress for "ideal" and "near ideal" temperature profiles

configuration, the J352, for similar effects since this is a configuration which has been used for a number of growth experiments. We will also examine the results of modifying lid and shield geometry with respect to temperature profile and minimizing stress generation.

3.2 Growth Velocity Experiments

Experiments with thinner lids to give greater growth speed were reported in the previous Quarterly Report [1]. It was found that in order to use these thinner lids, additional shielding was needed to maintain the slot region at a high enough temperature to prevent oxide accumulation. The presence of the additional shields, in turn, reduced the heat loss from the web so that the velocity benefit from the lids was compromised.

During the present reporting period, a modification of the thin lid concept -- the recessed lid -- was investigated. The philosophy behind the concept was that the slot region temperature is strongly influenced by heat conducted from the periphery of the lid where it is both in thermal contact with the susceptor and is also directly heated by induction. If the lid itself is thicker, then the conduction is enhanced and the slot region will be hotter. In a recessed lid, most of the lid is relatively thick to provide good thermal conduction, but the slot region is recessed to enhance the heat loss from the web. By using this approach, the temperature of the slot region can be kept high enough to prevent oxide build up without an excessive number of shields. Several conceptual designs are sketched in Figure 12.

Growth runs were made with recessed lids having configurations similar to the top two concepts in Figure 12. The thick portion of the lids were about 9.5 mm, while the recessed sections ranged from 5.6 mm to 3.2 mm. As expected, there were no significant problems with oxide accumulation. Further, thinning the recessed section did improve the speed characteristics of the lid, although not as much as hoped. As with the thin, uniform thickness lids, the effect of top shield configuration became dominant when the recessed section was thinner. Furthermore, growth

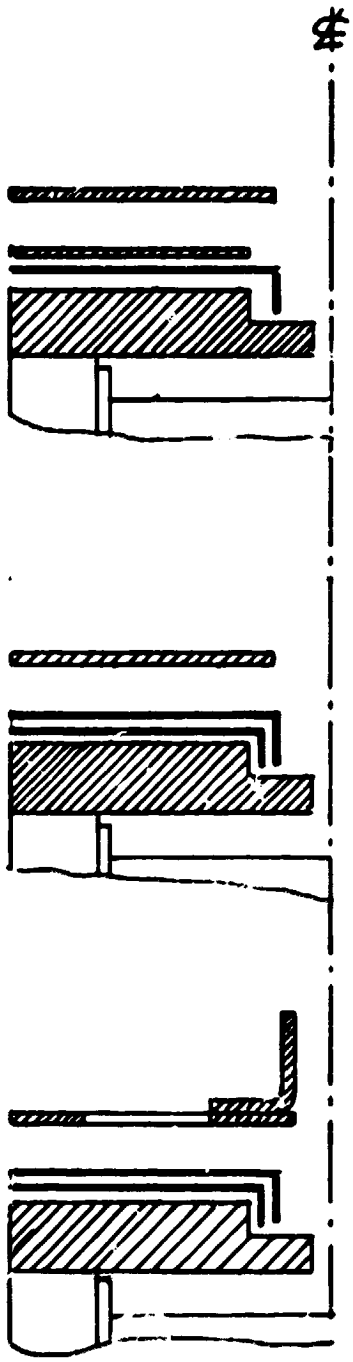

Figure 12 Design concepts for recessed lid configurations

difficulties, including high stresses, were enhanced when very thin recessed sections were used. Additionally, as has been noted in the past, one of the most important parameters in controlling the growth speed is the melt height. Again, the melt height interaction with the other geometrical factors was complex, and poor or difficult growth would occur when the melt was so high that the growth interface was probably well above the bottom of the lid.

The growth experiments with thin lids, recessed lids, and with a variety of shield geometries have re-emphasized the large number of parameters that influence the growth behavior of dendritic web. All these factors interact is a complex way to determine the growth speed and thermal stress in the growing ribbons. The experiments so far indicate that achieving any optimum configuration by empirical methods alone is difficult. It is expected that the thermal modeling results will be of great help in improving the growth speed as well as in reducing stress.

3.3 Melt Replenishment Experiments

While the final assembly of the electronic components of the melt level control system was taking place, growth experiments using manually set feed rates continued.

Lid and shield designs which provide width control were adapted for replenishment by the addition of feed and laser holes. This enabled the melt level to be maintained reasonably constant using a constant feed rate. Any mismatch between feed rate and consumption rate is manifested as a thickness variation in the crystal, so that any needed adjustments in feed rate can be made empirically. Thus growth at constant width allows growth experiments to be carried out at nearly constant melt level without the need for melt level sensing, at least over periods of several hours. It was also established that the width-limiting lid and shield designs continued to carry out their function in a melt replenishment configuration. Crystals up to 4 meters long were grown with manual replenishment.

Although the standard rectangular crucible design has performed well, it has become increasingly apparent that a longer crucible would be desirable in order to provide more physical space in which to separate the thermal requirements for growth of wide crystals and replenishment at the higher rates required to maintain a constant throughput. A new rounded-end crucible was designed and fabricated. This crucible has the same shape as the susceptor, i.e.,the geometry follows the susceptor perimeter. This design adds nearly 5 cm of useful length along the crucible center line with no change in the furnace configuration except the shape of the recessed portion of the susceptor. Initial tests of growth behavior in the elongated crucible did not show any inherent problems, but the thermal characteristics of this configuration are somewhat different from those of the shorter rectangular configuration. Recent work has therefore been directed toward a determination of optimum shielding, coil height,and crucible barrier positioning for good crystal growth with replenishment at full replacement rates.

Testing of the melt level control system during actual growth runs using the elongated configuration has begun. The precision with which the melt level can be detected was observed to be $\pm$ 0.1mm. The gain of the system is such that a decrease in melt level of 3.3 mm is required to alter the silicon feed rate from 0 g/min to a maximum of 0.91 g/min. This is accomplished by varying the speed of the gearmotor which turns the pellet feed mechanism from zero to a maximum of 7.7 rpm. With each motor revolution, four silicon pellets, each weighing approximately 0.03 g, are fed into the melt.

The procedure for setting up the system prior to a growth run is as follows. With an initial charge of silicon melted in the crucible, the silicon photodiode detector is positioned so that the reflected laser beam strikes the detector near its center. The bipolar output from the detector amplifier is thereby set to zero. An intentional offset is then introduced into the output amplifier which drives the gearmotor controller. The magnitude of this offset is chosen to match approximately the rate at which silicon will be removed from the melt during steady state growth.

During the test runs the value of the offset was 1.2 volts, which corresponds to a silicon withdrawal rate of 0.2 g/min.

Because the thermal trim changes needed for the new crucible design were not yet optimized nor had optimum positions for crucible barriers been determined, the growth conditions, independent of melt replenishment, were not as stable as we might wish during these tests, causing occasional growth termination by pull-out. However, it was established that the melt level control system operated overall as designed. This was established by recording both the output from the detector amplifier and the output from the motor controller (input to the pellet feed motor) and observing changes with changes in melt level. One change which we deem desirable is to lengthen the time constant in the control system in order to reduce the noise generated by the shimmering melt. This noise tends to apply an average upward bias to the feed rate. We plan to design and build a circuit which will provide a selection of time constants covering a wide range for experimental evaluation.

3.4 Experimental Web Growth Machine

Work in design, fabrication and assembly of a new experimental web growth machine is progressing as planned. The detailed mechanical design drawings are complete and general assembly drawings are being prepared. Fabrication of mechanical parts is underway and assembly of minor components is in progress. All components bought outside have been ordered.

The detailed electronic design is complete in informal format. Formal detailed circuit design drawings are being prepared. Informal design drawings of panel layouts have been prepared and fabrication is in progress. All electronic components to be purchased outside have to be placed on order. Assembly has begun.

3.5 Silicon Web Economic Analysis Update

The silicon web IPEG economic projection for 1986 has been updated to include cost adjustments for crucibles, labor rate and electric power rates. Costs are in 1980 dollars and include the following IPEG coefficients: EQPT-0.54, SQFT-110.6, DLAB-2.8, MATS-1.2, UTIL-1.2. The cost breakdown for a 3-day growth cycle is

EQPT = .54 x $15,600	$8424
SQFT = 110.6 x 30	3318
DLAB = 2.8 x 4 hrs/run x $6.30/hr x 117 runs/yr	8256
MATS = 1.2 [$20+(68 hrs/run x $.06/hr)] x 117	3381
UTIL = 1.2 x 3kW x 68 x $.05/kWh x 117	1432
Annual cost per furnace	$24,811
QUAN (annual output per furnace)	1153M^2
Area cost = $24,811/1153	21.52/M^2
Value added cost = $21.52/(1000 x .15 x .95)	15.1¢/Wpk
Polysilicon cost at $14.00/kG	3.9¢/Wpk
TOTAL SHEET COST	19.0¢/Wpk

This projection of 19 cents per peak watt is 1.7¢/Wpk higher than the previous projection but well below the JPL 1986 goal of 22.4¢/Wpk.

4. CONCLUSIONS

Stress buckling analysis has been applied to a specific lid and shield configuration, the J-181, and the modeling results agree with the growth experience. Both width and thickness effects have been analyzed and critical values determined. Having established confidence in the model, it will be applied to other configurations in order to define configuration elements which produce temperature distributions in the web which approach as closely as possible at zero stress profile and thus minimize buckling stresses in the growing web crystal.

A systematic series of experiments was carried out using recessed lids. Such lids combine some of the desirable features of thick lids in terms of quality of growth and thin lids in terms of growth velocity. A variety of top shield configurations was tested in order to evaluate the effects on both velocity and stress when lids with thin sections at the slot region are used. Growth behavior was found to be more sensitive to top shield configuration with thin lid sections than with thicker ones.

The melt level sensing system was tested during growth and performed as designed. Evaluations of an elongated crucible were also begun.

The design and construction of the new experimental web growth machine is proceeding on schedule.

5. PLANS FOR FUTURE WORK

During the coming quarter we will continue the modeling effort to aid the development of growth configurations which minimize buckling stress. Systematic experiments related to growth velocity will also continue. Experiments with growth in the elongated crucible with melt replenishment will also continue. Construction of the new experimental web growth machine will be completed.

6. NEW TECHNOLOGY

No new technology is reportable for the period covered.

7. REFERENCES

1. C. S. Duncan, et al., Large Area Sheet Task, Advanced Dendritic Web Growth Development, Quarterly Report, April 30, 1981. DOE/JPL 955843-81/2.

2. C. S. Duncan, et al., Silicon Web Process Development, Annual Report, June 30, 1980. DOE/JPL 954654-80/11.

3. C. S. Duncan et al., Silicon Web Process Development Annual Report, April 20, 1977 - April 19, 1979. Contract NAS 954654.

4. Boley, B. A. and Weiner, J. H., Theory of Thermal Stresses, p. 323, Wiley, New York, London, Sydney (1960).

5. Ibid.,p. 345.

6. C. S. Duncan et al., Large Area Sheet Task, Advanced Dendritic Web Development, Quarterly Report, January 31, 1981. DOE/JPL 954843-81/1

8. ACKNOWLEDGEMENTS

We would like to thank H. C. Foust, E. P. A. Metz, L. G. Stampahar, S. Edlis, W. B. Stickel, J. M. Polito, and W. Chalmers for their contributions to the web growth studies.

9. PROGRAM SCHEDULE AND COSTS

9.1 Updated Program Plan

9.1.1 Milestone Chart (attached)

9.1.2 Program Cost Summary (attached Curve 75242-A)

9.1.3 Program Labor Summary (attached Curve 725243-A)

9.2 Man-Hours and Costs

Man-Hours		Costs	
Previous	8,661	Previous	$384,346
This Period	4,799	This Period	244,928
Cumulative	13,460	Cumulative	629,274

LSA PROJECT

LARGE AREA SILICON SHEET

ADVANCED DENDRITIC WEB GROWTH DEVELOPMENT

MILESTONE CHART – JPL CONTRACT 955843

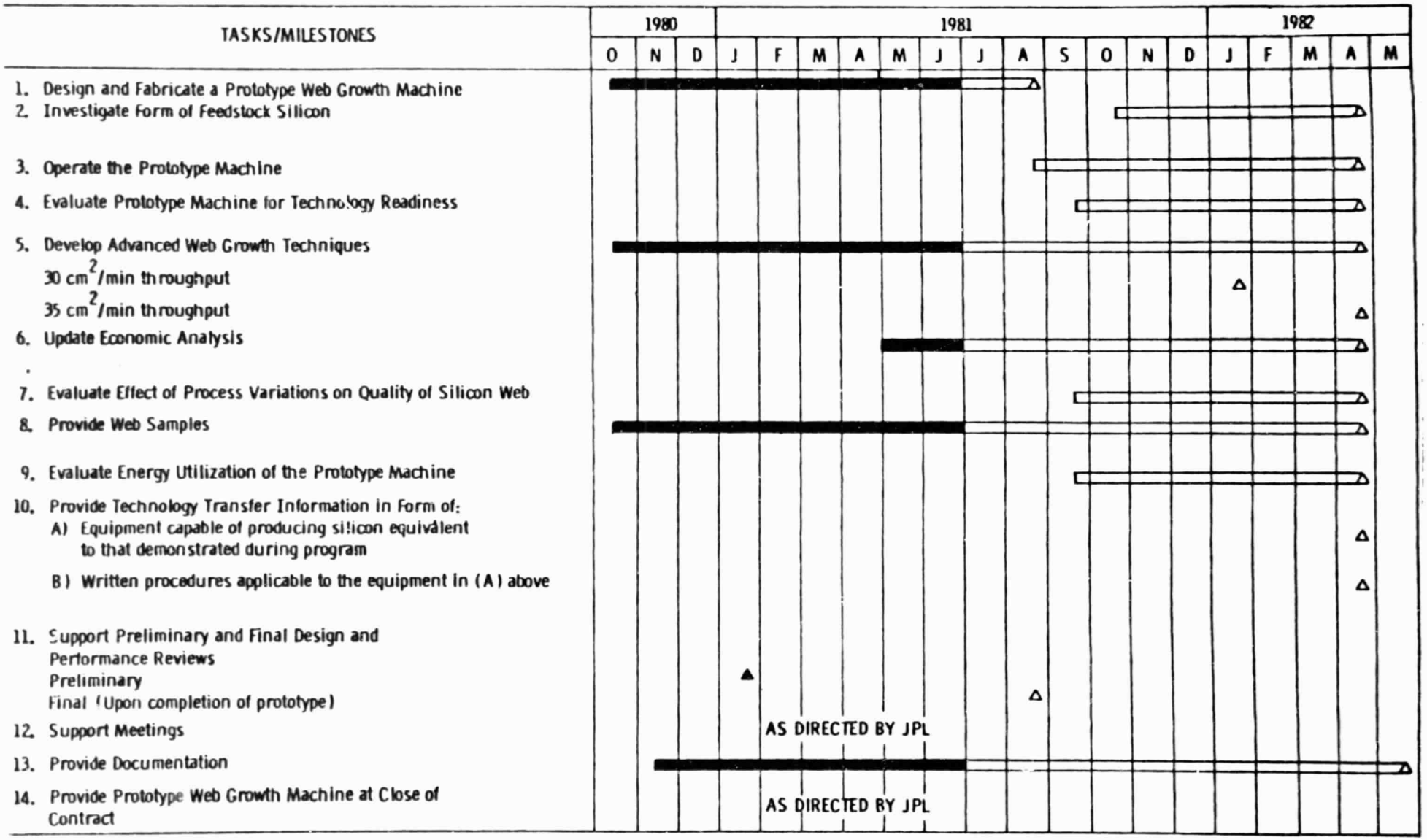

Curve 728214-8

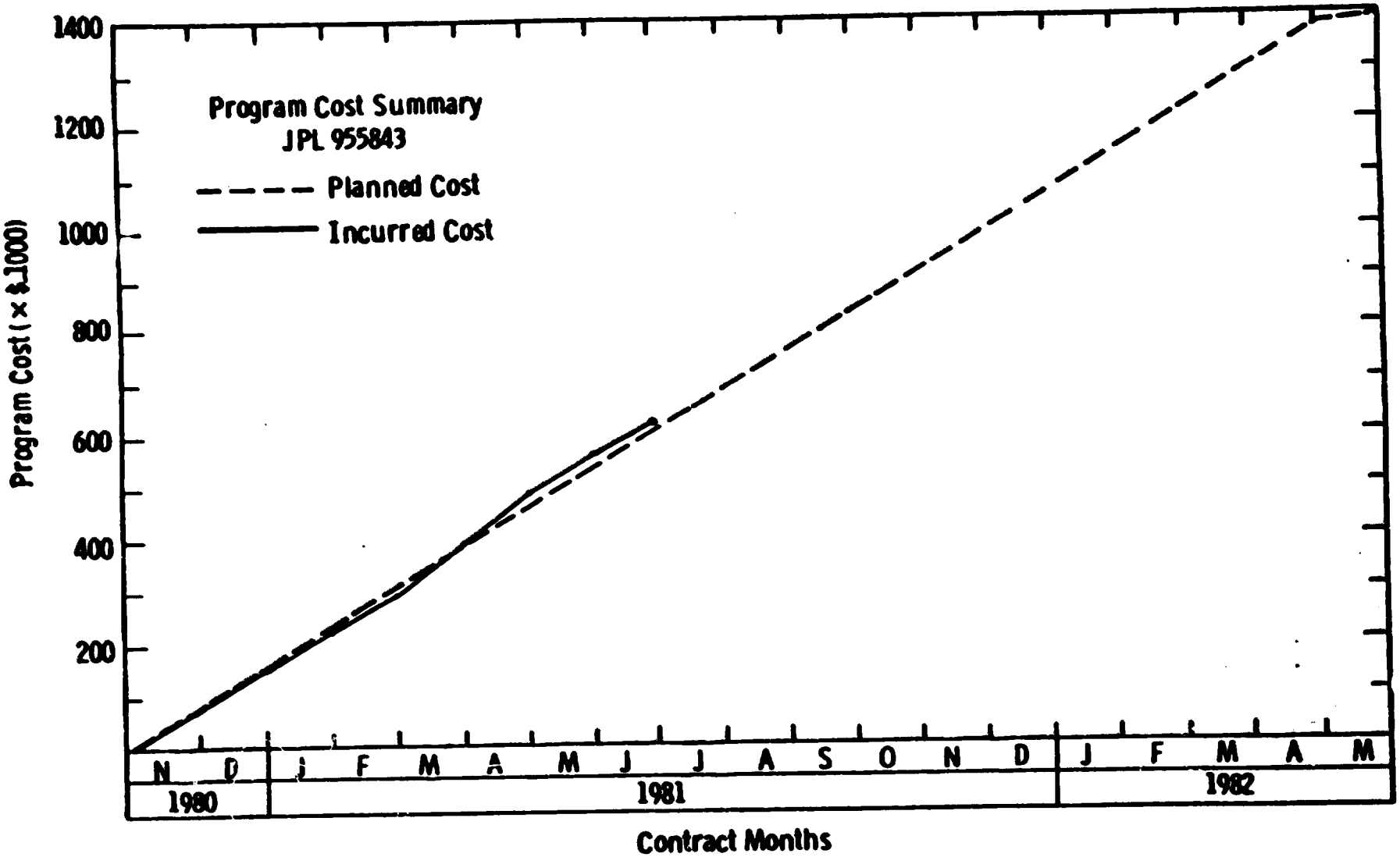

Curve 728215-B